A self-inactivating system for AAV-mediated *in vivo* base editing

Yuanbojiao Zuo
The Ohio State University
Peipei Wang
The Ohio State University https://orcid.org/0000-0003-1431-2139
Yandi Gao
The Ohio State University
Chen Zhang
The Ohio State University
Yuan Zhou
The Ohio State University
Haiwen Li
The Ohio State University
Zhiheng Chen
Central South University
zuocheng yang
the Third Xiangya Hospital, Central South University
Jie Xu
University of Michigan-Ann Arbor https://orcid.org/0000-0001-9452-2878
Jifeng Zhang
University of Michigan
Y. Chen
Division of Cardiovascular Medicine, Department of Internal Medicine, University of Michigan, Ann Arbor, MI, USA
Renzhi Han (renzhi.han@osumc.edu)
The Ohio State University https://orcid.org/0000-0002-8202-9186

Article

Keywords: AAV, ABE, adenine base editor, adeno-associated virus, base editing, cytosine base editor, CRISPR, hyperlipidemia, self-inactivating base editing

Posted Date: May 20th, 2022

DOI: https://doi.org/10.21203/rs.3.rs-1663604/v1

Abstract

DNA base editors have been harnessed as an exciting therapeutic platform for human diseases and are rapidly progressing into human clinical trials. However, persistent expression of base editors delivered via adeno-associated virus (AAV) poses concerns with specificity and immunogenicity. Here we develop self-inactivating base editor (siBE) systems with a negative feedback loop where one guide RNA (gRNA) targets the gene of interest and the other targets the deaminase domain itself. We demonstrate that siBE confers efficient on-target editing with time-dependent self-inactivation and increased editing specificity. For the *in vivo* utilization, we further employ the intein split approach to package siBE targeting mouse *Angptl3* into AAV9. Systemic delivery of AAV9-siBE confer efficient editing of *Angptl3* in liver, resulting in reduced serum levels of ANGPTL3, triglyceride and total cholesterol, with the active base editor undetectable at 8 weeks after administration. These self-inactivating base editing systems are highly promising for future therapeutic applications.

Introduction

DNA base editors can install point mutations in the genome without making double stranded DNA breaks (DSBs) and hold great promise for gene editing therapyc[1–3], as single-nucleotide variants (SNVs) account for half of known pathogenic genetic variants in human hereditary diseases[3]. A fast-growing body of studies have demonstrated the feasibility to correct disease-causing mutations in animal models using base editing, such as progeria[4], Duchenne muscular dystrophy (DMD)[5–8] and phenylketonuria[9]. Moreover, base editing was also shown to be highly efficient in editing cholesterol-regulating genes such as *PCSK9* in cynomolgus monkeys[10, 11], suggesting the broad therapeutic applications of base editing for genetic and metabolic diseases. Indeed, two companies, Beam Therapeutics and Verve Therapeutics have got the green light from the US Food and Drug Administration for their upcoming clinical trials[12].

Adeno-associated virus (AAV) is the most widely used delivery platform for *in vivo* gene therapy due to its broad tissue targeting capacity with high efficiency[13, 14] and non-pathogenicity without causing any known human diseases[15, 16]. Others and us recently showed highly efficient *in vivo* gene correction in various animal models of human diseases using intein-split base editors delivered via AAV[4, 5, 9]. However, persistent expression of genome editing reagents delivered through AAV may result in increased accumulation of unwanted off-target events[5, 17, 18], which poses a major safety concern for gene editing therapy. Moreover, long-term expression of bacteria-derived Cas9 protein has been shown to trigger the host immune responses, which may lead to the elimination of edited cells[19]. Therefore, it is crucial to limit the expression duration of gene editing reagents for future clinical applications. A self-cleaving approach has been reported to reduce the expression duration of Cas9 protein and improve the safety profile[20–23]. However, approaches to control the expression duration of base editors delivered in AAV have not yet been reported.

In this study, we developed self-inactivating adenosine base editor (siABE) and cytosine base editor (siCBE) systems with a negative feedback loop where one guide RNA (gRNA) targets the gene of interest and the other targets the deaminase domain itself. We demonstrated that both siABE and siCBE can confer efficient on-target editing with time-dependent self-inactivation. We further employed the Gp41-1 intein split approach[5] to package siCBE targeting mouse *Angptl3* into AAV9. Systemic delivery of AAV9-siCBE conferred efficient editing of Angptl3 in liver, resulting in reduced serum levels of ANGPTL3, triglyceride (TG) and total cholesterol (TC). Importantly, the functional base editor was not detectable in the liver at 8 weeks after administration. These self-inactivating base editing systems are highly promising for future therapeutic applications.

Results

Design and in vitro validation of siABE

The inherited DNA and RNA off-target activities of BEs are of concern for clinic applications. As the deaminase domains used in the BEs largely contribute to the observed off-target activities[24–26], we hypothesize that providing a negative-feedback gRNA targeting the deaminase domain used in BE would help to minimize such off-target activities. A previous study showed that the cysteine residue at position 90 (C90) residing near the enzymatic pocket of TadA* (Fig. 1A) appeared to be critical for its enzymatic function[27]. We first engineered ABE8e_V106W[28] with the C90R mutation and confirmed that the C90R mutation completely abolished its editing activity (Fig. 1B). We then designed a gRNA to install the C90R mutation in ABE8e_V106W. At three days after co-transfection of the C90-gRNA and ABE8e_V106W plasmids into Neuro-2a cells, the C90R editing efficiency was estimated to be around 67% by BEAT analysis of the ABE8e_V106W transcripts (Fig. 1C).

We previously developed a Gp41-1 intein split strategy to enable highly efficient assembly of full-length iABE-NGA and AAV packaging for *in vivo* base editing[5]. To test if incorporation of the C90-gRNA into the intein split would allow simultaneous editing of the target gene while disabling the ABE enzyme itself, we inserted the C90-gRNA expressing cassette into the N-terminal half of intein split plasmids along with a targeting gRNA for the gene of interest (eg. the *mdx*^{4cv}-gRNA) (Fig. 1D). To test the performance of this two-component siABE system, we co-transfected the HEK293 cells with the N-terminal, C-terminal and the BEON fluorescent reporter construct[29], which carries the *mdx*^{4cv} targeting sequence disrupting the downstream EGFP expression. The GFP fluorescence can be rescued by successful editing of ABE and corresponding target gRNA. As shown in Fig. 1E, transfection with the reporter alone resulted in minimal background fluorescence, while the cells co-transfected with all three plasmids, either with or without C90R gRNA, showed robust GFP fluorescence. FACS analysis showed that EGFP expression was restored to similar levels in the cells transfected with or without C90-gRNA (Fig. 1F). The editing rate was analyzed by BEAT analysis of the Sanger sequencing traces of the transcript amplicons. We found that the C90-gRNA did not significantly compromise the editing rate of the *mdx*^{4cv} target sequence as compared with the positive control group without the C90-gRNA (Fig. 1G). However, there was a time-dependent increase

in the C90R editing efficiency in the siABE-N/C transfected group (Fig. 1H), indicating that the negative feedback editing increasingly disables the ABE enzyme. We further tested the performance of siABE-N/C to edit an endogenous gene *Apoc3*, which encodes an inhibitor for lipoprotein lipase, in Neuro-2a (N2a) cells. Again, we observed no significant difference between ABE-N/C and siABE-N/C groups (Fig. 1I), suggesting that the C90-gRNA offers a simple approach to restrict the ABE activity without substantially compromising the editing of the target gene.

Design and in vitro validation of siCBE

Next, we took a similar approach to design a self-inactivating CBE (siCBE) system. We reasoned that CBE-mediated installation of a premature stop codon within the cytosine deaminase domain would switch off the CBE, thus providing a negative feedback loop for regulating the CBE activity. We designed a gRNA (Q125-gRNA) to install a premature stop codon at Q125 within the AncBE4 enzyme (Fig. 2A). Transfection of AncBE4 with the Q125-gRNA led to an average Q125X editing efficiency of 57.9% ± 5.5% (Fig. 2B). The installation of Q125X is predicted to gradually turn off the expression of AncBE4. To test this, we harvested the cells at 24, 48, 72 and 96 hours after transfection and analyzed the time-course expression of AncBE4 using the anti-Cas9 antibodies. The expression levels of both N-terminal and full-length AncBE4 were not significantly different between CBE and siCBE groups when examined at 24 hours (Fig. 2C, D). However, both the full-length and N-terminal AncBE4 was decreased more rapidly in cells transfected with siCBE starting from 48 hours when compared with the CBE group (Fig. 2C, D). Consistently, there was a time-dependent increase in the Q125X editing in the AncBE4 transcript (Fig. 2E). To test whether the addition of the Q125-gRNA in siCBE impairs the editing activity at an endogenous locus, we compared the editing efficiency at HEK4 site between the CBE and siCBE in HEK293 cells. The siCBE showed only a slight, but statistically insignificant, decrease in the editing efficiency as compared with CBE (Fig. 2F).

As different cytosine deaminase domains have been utilized in engineered CBEs, we tested a similar approach to develop siCBE-evoFERNY that carries a smaller evolved deaminase evoFERNY[30]. A W65-gRNA was designed in order to introduce a premature codon into tryptophan at 65 (W65) within evoFERNY. As described above for siCBE, we observed a time-dependent increase of editing efficiency at W65 of evoFERNY in siCBE-evoFERNY transfected cells (Fig. 3A). Western blot showed that the full-length CBE-evoFERNY expression decreased more rapidly in the siCBE-evoFERNY group than the canonical CBE-evoFERNY (Fig. 3B). To test if introduction of the self-targeting W65-gRNA may affect the performance of the target gRNA for the gene of interest, we inserted a gRNA targeting mouse *Asgr1* to install a loss-of-function (LoF) mutation at the codon W158. It was recently shown that the LoF variants of human *ASGR1* are associated with lower levels of non-HDL cholesterol[31]. The siCBE-evoFERNY achieved an average editing rate of 16.9% ± 1.0%, a small but significant decrease when compared with canonical CBE-evoFERNY (23.1% ± 2.0%, $p = 0.003$) (Fig. 3C).

Next, we attempted to further design the C-terminal half construct by adding the self-inactivating gRNA target sequence into the coding region of siCBE-C (siCBE-v2) in order to achieve simultaneous

inactivation of both N- and C-terminal fragments (**Supplementary Figure S1A**). After transfection of the siCBE-v2 into HEK293 cells, we performed Western blot analysis at different time points to examine the inactivation of N-, C- and full-length CBE expression. As shown in **Supplementary Figure S1B**, we found that the C-terminal half and the full-length CBE were efficiently switched off. But surprisingly, we observed that inactivation of N-terminal half was not as efficient as the siCBE. We thus chose siCBE for further *in vivo* studies.

Design and in vitro studies of gRNA targeting Angptl3

Genome-wide association studies (GWAS) have linked a number of LoF variants in several genes to favorable lipid profile and reduced cardiovascular diseases, such as *PCSK9*, *ANGPTL3*[23], *APOC3*[24] and *ASGR1*[26], making them attractive therapeutic targets for hypercholesterolemia. To assess the *in vivo* performance of siBE, we chose *ANGPTL3* as a therapeutic target with the goal to develop a “one shot, one cure” treatment for hypercholesterolemia as a monoclonal antibody against ANGPTL3 has recently been approved by FDA. We first designed several gRNAs to install either a premature stop codon or disrupt the canonical splicing donor (SD, e.g. GT dinucleotide) or acceptor (SA, e.g. AG dinucleotide) sequences into mouse *Angptl3* using CBE or ABE. To install the Q135X premature stop codon (Q135X) into the coding sequence of mouse *Angptl3*, two overlapping gRNAs (gRNA1 and gRNA2) with different PAM sequences (GGG or GGC) were constructed (Fig. 4A). Transfection of N2a cells with the gRNAs and their corresponding CBEs (e.g. AncBE4 for gRNA1 and CBEmax-SpG for gRNA2) induced efficient installation of Q135X mutation in *Angptl3* (Fig. 4B). The gRNA1 and AncBE4 combination induced 51.5 ± 8.0% conversion of C to T at the Q135 codon, while the efficiency of gRNA2 and CBEmax-SpG was slightly lower (40.0 ± 0.8%). We also designed a gRNA (E4-gRNA) to mutate the exon 4 SD site of mouse *Angptl3* in combination with either CBEmax-SpG (IVS4 + 1G > A) or ABE8eV106W-SpG (IVS4 + 2T > C) (Fig. 4A). While CBEmax-SpG showed little editing efficiency to induce IVS4 + 1G > A conversion, ABE8eV106W-SpG induced 19.0 ± 3.9% editing to install IVS4 + 2T > C mutation at this SD site (Fig. 4C). Based on these data, we chose the gRNA1, which showed the highest editing efficacy, for the downstream experiments. We inserted two copies of the gRNA1 into the siCBE-N construct and compared the editing efficiency of siCBE with that of the canonical CBE for editing *Angptl3*. There was no significant different between siCBE and CBE groups (Fig. 4D).

In vivo performance of AAV9-siCBE/Angptl3 in mice

To test the performance of siCBE *in vivo*, we chose AAV9 as a delivery method and *Angptl3* as the target gene. We packaged the two Gp41-1 intein split halves of the siCBE/Angptl3 into AAV9 (Fig. 5A) and tested if *in vivo* delivery of AAV9-siCBE could reduce the lipid profile in mice. The N-terminal vector carries two copies of Angptl3 gRNA1 under the control of human U6 promoter and AncBE4 split at 513 fused with the C-terminus of Gp41-1 intein driven by a liver-specific promoter human alpha-1-antitrypsin [hAAT][32–34]. The C-terminal vector carries the self-targeting Q125X-gRNA and the N-terminal Gp41-1 intein fused with the second half of AncBE4 split driven by hAAT promoter. Both vectors are within the packaging capacity of AAV and packaged efficiently.

We treated six wild-type (WT, C57BL/6J) mice with AAV9-siCBE/Angptl3 (a total of 2 x 10^{14} vg/kg, 1:1 of the N and C-terminal half) through the tail vein injection at 6 weeks of age. Two additional mice receiving either the N-terminal half or the C-terminal half alone were used as negative control. We measured serum levels of Angptl3, triglyceride (TG) and total cholesterol (TC) at different time points after AAV9-siCBE/Angptl3 administration. Compared with the control mice, all AAV9-treated animals exhibited dramatically decreased ANGPTL3 protein levels at one week after the treatment (after: 15.4 ± 6.3 ng/ml vs control: 100.7 ± 24.8 ng/ml), which remained low at 4 and 8 weeks after treatment (Fig. 5B). Similarly, AAV9-siCBE/Angptl3 treatment dramatically reduced the TG levels in all animals at 1–8 weeks after treatment (Fig. 5C). The TC levels were also significantly reduced by AAV9-siCBE/Angptl3 treatment (Fig. 5D).

We quantified the gene editing efficiency in the liver samples from the treated mice at 8 weeks after treatment. Sequencing of the *Angptl3* transcript amplicons from the treated animals showed an average of 56.9% ± 18.0% C to T editing at the codon Q135 (Fig. 5E). Sequencing of the genomic DNA from the liver samples showed a similar editing efficiency (57.8% ± 3.8%) at the target site (Fig. 5F). We also amplified the AncBE4 transcript from the treated animals and sequencing showed an average of 77.7% ± 4.0% editing while the mouse treated with the N-terminal half alone showed undetectable editing as expected. To further examine whether the editing of AncBE4 disrupted the expression of AncBE4, we performed Western blot analysis of the liver tissues at 8 weeks after AAV9 treatment with the anti-Cas9 antibody, which recognizes the N terminus of Cas9. As shown in Fig. 5H, both the N-terminal and full-length AncBE4 were not detected in mice treated with AAV9-siCBE/Angptl3, whereas the N-terminus of AncBE4 was readily detectable in the mouse treated with the N-terminal half alone. Taken together, these results suggest that the AAV9-delivered siCBE/Angptl3 induced highly efficient editing of *Angptl3* and its own transcript.

Off-target activities

A major advantage of the siBE system versus the conventional BE is that it would eliminate the deaminase domain-mediated nonspecific RNA editing as it efficiently switched off the expression of deaminase domain-containing fragment (see Fig. 5). We reasoned that the reduced expression duration of the functional base editor in the siBE system may also reduce the off-target DNA editing activity. To test this, we chose several previously validated off-target sites conferred by the HEK4 gRNA[30]. CBE or siCBE plus HEK4 gRNA were co-transfected into HEK293 cells and the off-target sites were amplified by PCR. As shown in Fig. 6A, while there was no significant difference for on-target editing of HEK4 site between the CBE and siCBE groups, siCBE exhibited significantly lower C5 editing at the off-target site 1 (OT1) (16.4 ± 0.7%, $p < 0.001$) compared to CBE (22.7 ± 1.3%). At OT2, both siCBE and CBE showed background levels of editing activities. Similarly, we analyzed the HEK4-OT4 site and found siCBE generated slightly lower, insignificant editing rate at C6 compared to CBE group.

The siBE system requires both a therapeutic gRNA and a self-targeting gRNA, which may lead to additional off-target activities in the genome[20, 22, 35]. To test the off-target activities of both Angptl3-

Q135X gRNA and the self-targeting Q125X gRNA in mouse genome, we examined the top putative off-target sites predicted by the Cas-OFFinder[36]. We transfected N2a cells with CBE or siCBE constructs, amplified the off-target sites by PCR and subjected the amplicons to Sanger sequencing. None of the top predicted off-target sites of Angptl3-Q135X gRNA and the self-targeting Q125X gRNA showed detectable off-target activities (Fig. 6B**&C**). Similarly, we also measured the off-target activities in mouse livers following AAV9-siCBE/Angptl3 treatment. We observed undetectable off-target activities at four of the five off-target sites in the treated mice (Fig. 6D**&E**). These results suggest that the siCBE conferred highly specific editing in *in vitro* and *in vivo* settings.

Discussion

In sum, we have developed generalizable siBE systems that confer efficient on-target editing with reduced off-target activity when compared with conventional BE. Through the addition of a self-inactivating gRNA, our simple siBE systems reduced the off-target activity by limiting the duration and concentration of BE expression and obviated the needs of large regulatory sequences, chemical or physical stimuli, or sophisticated engineering. Systemic AAV9-mediated delivery of siCBE resulted in efficient editing of *Angptl3* in mouse liver, which functionally reduced the serum levels of ANGPTL3 protein, TG and TC with the functional base editor protein eliminated when examined at 8 weeks after delivery. To the best of our knowledge, this is the first report of self-inactivating BE systems that can be switched off at the transcription level without external triggers and can be delivered by AAV for *in vivo* base editing. These siBE systems hold tremendous promise in clinical translation.

The base editing has emerged as a powerful tool for correction of the pathogenic mutations[1, 2, 37]; however, off-target effects are the major safety concern for clinical applications of this revolutionary technology. Previous studies have shown that continuous exposure to base editors resulted in increased accumulation of the off-target activity[25, 26, 38–40]. The use of ribonucleoprotein (RNP)[41–43] or mRNA[44–46] delivery instead of DNA delivery has been shown to effectively reduce the off-target activity. Although highly promising for diseases that require only localized tissue delivery, it is still highly challenging to deliver the RNP or mRNA systemically to achieve high efficiency of body-wide gene editing as required for many diseases such as muscular dystrophy. Alternatively, temporal control of base editors can be achieved by incorporating an inducible promoter[47] or an inducible assembly of functional enzymes from inactive fragments[48, 49]. The former works at the transcriptional level but requires introduction of large regulatory sequences and/or additional transcriptional factors, which pose additional constraints considering the limit packaging capacity of AAV. The latter achieves inducibility by splitting the deaminase domains into two inactive components, which can be assembled into a functional format with a chemical inducer.

Both approaches often exhibit leaky background expression or editing and require additional chemical inducers, which may pose additional cytotoxicity. Moreover, neither has been tested for *in vivo* base editing. In contrast, our siBE systems achieve temporal control by the use of a self-inactivating gRNA

expression cassette, which adds only about 360 bp in length. However, the introduction of the self-inactivating gRNA may lead to additional off-target activities, which can be mitigated by careful design and rigorous *in vitro* validation.

Another potential issue with our siBE strategy is that the self-inactivating gRNA may outcompete for the base editor, thus reducing the on-target editing of the therapeutic gene. Our results suggest that this is generally not an issue, but we indeed noticed in one case that the siCBE-evoFERNY showed a reduced activity for editing *Asgr1* as compared to the conventional CBE-evoFERNY (Fig. 3C). Although not tested, we envision that introducing a mismatch on the self-inactivating gRNA may lower down its efficacy or choosing a different gRNA for the therapeutic gene may help to achieve higher efficient therapeutic editing. In addition, our attempt to generate siCBE-v2 with the self-inactivating gRNA target sequence incorporated in both the N- and C-constructs led to inefficient inactivation of the N-terminal half, further highlighting the importance of carefully designing the self-inactivating gRNA and therapeutic gRNA to achieve a balanced editing at the BE coding sequence and therapeutic locus.

Finally, our work demonstrates for the first time that AAV9-mediated delivery of siCBE targeting *Angptl3* can effectively reduce the blood lipid levels. The expression of *Angptl3* is restricted to the liver, an ideal target organ for in *vivo* genome editing due to the tissue accessibility by intravenous administration. Also, various LoF mutants of *ANGPTL3* have been identified in human population without major adverse health consequences[50–53] and genetic disruption of *Angptl3* in mice corroborated this finding. Thus, it has become a promising therapeutic target for lipid control. We observed that AAV9-siCBE/Angptl3 achieved an average editing of 57.8% ± 1.5% at *Angptl3* target site with concomitant reduction in the serum TG and TC levels and minimal off-target activities, supporting the clinical translation of targeting *ANGPTL3* with base editing for lipid control.

Materials And Methods

Mice

Mice (C57BL/6J) were purchased from the Jackson Laboratory and housed at The Ohio State University Laboratory Animal Resources in accordance with animal use guidelines. All the experimental procedures were approved by the Animal Care, Use, and Review Committee of the Ohio State University. All mice were maintained under standard conditions of constant temperature (72 ± 4°F), humidity (relative, 30–70%), in a specific pathogen-free facility and exposed to a 12-h light/dark cycle.

Cell culture and transfection

HEK293 and N2a cells were maintained in Dulbecco's Modified Eagle Medium (DMEM) (Fisher Scientific, 11-965-092) with 10% FBS and 1% 100X penicillin-streptomycin (Thermo Fisher Scientific, 15140122) in 10-cm dishes. Medium were change every two days or as needed. Cells were seeded in 6-well plates and transfected with 2 μg plasmids (1:1 for gRNA and base editor, or 1:1 N- and C-terminal constructs) when

cell density reached ~ 70% confluency. The transfection was conducted by XtremeGENE HP DNA transfection reagent (MilliporeSigma #6366546001) according to manufacturer's protocol.

Plasmid construction

Complete DNA sequences for plasmids and the primers used are provided in the **Supplementary Table S1**.

All gRNA plasmids were constructed by annealing the oligos and ligated into pLenti-ogRNA or the corresponding split base editor constructs as described below.

ABEmax7.10_SpG and CBE4max-SpG were kind gifts from Benjamin Kleinstiver (Addgene: #140002 and #139998). ABE8eV106W-SpCas9 and AncBE4max and were kind gifts from David Liu (Addgene: #138495 and #112094). ABE8eV016W-SpG, iABE-NGA Gp41-1 splits (N and C) and the *mdx*^{4cv} BEON reporter were described previously [5, 29]. ABE8eV106W(C90R)-SpG was constructed by fusion PCR. All Gp41-1 intein split of siABE or siCBE constructs were constructed based on the splits of iABE-NGA. hAAT promoter was PCR amplified from the genomic DNA of HEK293 cells and subcloned into the corresponding N and C terminal constructs of siCBE.

Flow cytometry

HEK293 cells were harvested and re-suspended in MACS buffer (Miltenyi Biotec, 130-091-221) at 72 hours after transfection. A total of 10,000 cells were collected by Becton Dickinson LSR II with BD FACSDiva software version 8.0.1 (BD Biosciences) to determine GFP-positive cells. Data was analyzed using FlowJo 10.4 software. The gating strategy is shown in **Supplementary Figure S2**.

Genomic DNA and total RNA extraction, PCR and Sanger Sequencing

Genomic DNA was extracted using DNA lysis buffer (100 mM Tris-Cl pH 8.0, 50 mM EDTA and 1% SDS) with proteinase K according to manufacturer's instruction. Total RNA was extracted using Quick-RNA MiniPrep Kit (ZYMO Research, R1055). RT-PCR was conducted using RevertAid RT Reverse Transcription Kit (Thermo Fisher Scientific, K1691) with 100 ng RNA as template. The cDNA (1 µl) or genomic DNA (100 ng) was amplified using GoTaq Master Mix (Promega, M7122). The PCR products were purified by Wizard SV Gel and PCR Clean-Up System (Promega, A9285) according to manufacturer's protocol. Purified products were subjected to Sanger sequencing at the Genomics Shared Resource of the Ohio State University Comprehensive Cancer Center and analyzed by BEAT program.

Generation of AAV particles

AAV vectors were produced at the viral vector core of the Nationwide Children's Hospital[54]. The siCBE-N and C constructs were packaged into AAV9 capsid using the standard triple transfection protocol[55]. AAV9-siCBE-N and C were titered using digital droplet PCR. Titers are expressed as DNase resistant particles in vector genome per ml (vg/ml) and rAAV titers used for injection in mice were 2.7 x 10^{13} vg/ml for AAV9-siCBE-N and 3.0 x 10^{13} vg/ml for AAV9-siCBE-C.

Tail vein injection of AAV9 particles

AAV9-siCBE-N/C viral particles (total: 2 x 10^{14} vg/kg, 1:1 of N and C) were systemically injected into C57BL/6J mice at 6 weeks of age through tail vein injection as described previously[5].

Measurement of serum lipid profile and ANGPTL3

Blood samples were obtained from the facial vein and allowed for clotting at room temperature for 10–30 min. Serum samples were collected after centrifugation at 5000 rpm for 10 min and stored at -80°C. The TG and TC levels were measured using the triglyceride and cholesterol assay kit (Abcam, ab65336&ab65390) according to the manufacture's protocol. The serum ANGPTL3 protein level was measured using the mouse Angiopoietin-like 3 quantikine ELISA Kit (R&D Systems, MANL30) according to the manufacture's protocol.

Western blot analysis

Cells were lysed with cold RIPA buffer supplemented with 1x protease inhibitor. Protein samples were separated using 4–15% SDS-PAGE gel (Bio-Rad, 17000927) and transferred onto 0.45 μM PVDF membrane. The rabbit polyclonal anti-Cas9 (Diagenode, C15310258-100, 1:2000), mouse polyclonal anti-Cas9 C-terminal (Diagenode, C15200231-100, 1:2000) and rabbit monoclonal anti-GAPDH (2118S, 1:2000, Cell Signaling Technology, 2118S, 1:2000) antibodies were used for immunoblotting analysis. HRP conjugated goat anti-mouse (7076S, 1:4000) and goat anti-rabbit (7074S, 1:4000) secondary antibodies were obtained from Cell Signaling Technology, Danvers, MA. The membranes were developed using ECL Western blotting substrate (Pierce Biotechnology, Rockford, IL) and scanned by ChemiDoc XRS + system (BioRad, Hercules, CA). Results were quantified using Image Lab 6.0.1 software (Bio-Rad Laboratories, Hercules, CA) according to the manufacturer's instruction.

Statistical Analysis

The data are expressed as the mean ± SD and analyzed by GraphPad Prism v.8.0.1 (GraphPad Software). Statistical differences were determined by two-tailed unpaired Student's *t* test for two groups and one-way ANOVA with Turkey's post tests for multiple group comparisons. A p value < 0.05 was considered as significant.

Abbreviations

AAV: Adeno-associated virus

Angptl3: angiopoietin like 3

Apoc3: apolipoprotein C3

Asgr1: asialoglycoprotein receptor 1

DMD: Duchenne muscular dystrophy

DSBs: double stranded DNA breaks

GFP: green fluorescent protein

gRNA: guide RNA

hAAT: human alpha-1-antitrypsin

OT: off-target

Pcsk9: proprotein convertase subtilisin/kexin type 9

RNP: Ribonucleoprotein

SD: splicing donor

siABE: self-inactivating adenosine base editor

siCBE: self-inactivating cytosine base editor

SNVs: single-nucleotide variants

TC: total cholesterol

TG: triglyceride

Declarations

Ethics approval and consent to participate

Not applicable.

Consent for publication

All co-authors have reviewed and approved of the manuscript prior to submission. The manuscript has been submitted solely to this journal and is not published, in press, or submitted elsewhere.

Availability of data and material

All relevant data supporting the key findings of this study are available within the article and its Supplementary Information files or from the corresponding author upon reasonable request.

Author Contributions

R.H. conceived the study and wrote the manuscript. Y.Z. performed the experiments and participated in drafting the manuscript. P.W. assisted with FACS and Y.G. assisted with blood collection. C.Z. and Y.Z. assisted in the Western blot analysis of siCBE-v2. All authors contributed to the final version of the manuscript.

Acknowledgements

The authors would like to thank all lab members for their constructive comments and suggestions. The authors thank the Viral Vector Core at the Nationwide Children's hospital for producing the AAV, the Analytical Cytometry Shared Resource of the Ohio State University Comprehensive Cancer Center for FACS, the Genomics Shared Resource of the Ohio State University Comprehensive Cancer Center for sequencing.

Competing interests

The authors (R.H., Y.G. and L.X.) have submitted a patent application based on the results reported in this paper. All other authors confirm no other conflicts of interest.

Funding

R.H. is supported by US National Institutes of Health grants (R01HL116546, R01HL159900, R01AR070752), a Parent Project Muscular Dystrophy award and Miao family gift. R.H. has received commercial research support from Stealth Biotherapeutics.

References

1. Gaudelli, N.M. et al. Programmable base editing of A*T to G*C in genomic DNA without DNA cleavage. Nature **551**, 464–471 (2017).
2. Komor, A.C., Kim, Y.B., Packer, M.S., Zuris, J.A. & Liu, D.R. Programmable editing of a target base in genomic DNA without double-stranded DNA cleavage. Nature **533**, 420-+ (2016).
3. Porto, E.M., Komor, A.C., Slaymaker, I.M. & Yeo, G.W. Base editing: advances and therapeutic opportunities. Nat Rev Drug Discov **19**, 839–859 (2020).
4. Koblan, L.W. et al. In vivo base editing rescues Hutchinson-Gilford progeria syndrome in mice. Nature **589**, 608–614 (2021).

5. Xu, L. et al. Efficient precise in vivo base editing in adult dystrophic mice. Nature communications **12**, 3719 (2021).
6. Ryu, S.M. et al. Adenine base editing in mouse embryos and an adult mouse model of Duchenne muscular dystrophy. Nature biotechnology **36**, 536–539 (2018).
7. Chemello, F. et al. Precise correction of Duchenne muscular dystrophy exon deletion mutations by base and prime editing. Science advances **7** (2021).
8. Li, J. et al. Therapeutic Exon Skipping Through a CRISPR-Guided Cytidine Deaminase Rescues Dystrophic Cardiomyopathy in Vivo. Circulation **144**, 1760–1776 (2021).
9. Villiger, L. et al. Treatment of a metabolic liver disease by in vivo genome base editing in adult mice. Nat Med **24**, 1519–1525 (2018).
10. Musunuru, K. et al. In vivo CRISPR base editing of PCSK9 durably lowers cholesterol in primates. Nature **593**, 429–434 (2021).
11. Rothgangl, T. et al. In vivo adenine base editing of PCSK9 in macaques reduces LDL cholesterol levels. Nature biotechnology **39**, 949–957 (2021).
12. Eisenstein, M. Base editing marches on the clinic. Nature biotechnology (2022).
13. Naso, M.F., Tomkowicz, B., Perry, W.L., 3rd & Strohl, W.R. Adeno-Associated Virus (AAV) as a Vector for Gene Therapy. BioDrugs **31**, 317–334 (2017).
14. Fraldi, A. et al. Gene therapy for mucopolysaccharidoses: in vivo and ex vivo approaches. Ital J Pediatr **44**, 130 (2018).
15. Lykken, E.A., Shyng, C., Edwards, R.J., Rozenberg, A. & Gray, S.J. Recent progress and considerations for AAV gene therapies targeting the central nervous system. J Neurodev Disord **10**, 16 (2018).
16. Wang, D., Tai, P.W.L. & Gao, G. Adeno-associated virus vector as a platform for gene therapy delivery. Nat Rev Drug Discov **18**, 358–378 (2019).
17. Zhang, J., Chen, L., Zhang, J. & Wang, Y. Drug Inducible CRISPR/Cas Systems. Comput Struct Biotechnol J **17**, 1171–1177 (2019).
18. Nelson, C.E. et al. Long-term evaluation of AAV-CRISPR genome editing for Duchenne muscular dystrophy. Nat Med **25**, 427–432 (2019).
19. Rees, H.A. & Liu, D.R. Base editing: precision chemistry on the genome and transcriptome of living cells. Nat Rev Genet **19**, 770–788 (2018).
20. Chen, Y. et al. A Self-restricted CRISPR System to Reduce Off-target Effects. Mol Ther **24**, 1508–1510 (2016).
21. Petris, G. et al. Hit and go CAS9 delivered through a lentiviral based self-limiting circuit. Nat Commun **8**, 15334 (2017).
22. Wang, H. et al. Development of a Self-Restricting CRISPR-Cas9 System to Reduce Off-Target Effects. Mol Ther Methods Clin Dev **18**, 390–401 (2020).
23. Li, Q. et al. In vivo PCSK9 gene editing using an all-in-one self-cleavage AAV-CRISPR system. Mol Ther Methods Clin Dev **20**, 652–659 (2021).

24. Jeong, Y.K., Song, B. & Bae, S. Current Status and Challenges of DNA Base Editing Tools. Mol Ther **28**, 1938–1952 (2020).
25. Park, S. & Beal, P.A. Off-Target Editing by CRISPR-Guided DNA Base Editors. Biochemistry **58**, 3727–3734 (2019).
26. Yu, Y. et al. Cytosine base editors with minimized unguided DNA and RNA off-target events and high on-target activity. Nat Commun **11**, 2052 (2020).
27. Grunewald, J. et al. CRISPR DNA base editors with reduced RNA off-target and self-editing activities. Nature biotechnology **37**, 1041–1048 (2019).
28. Richter, M.F. et al. Phage-assisted evolution of an adenine base editor with improved Cas domain compatibility and activity. Nature biotechnology **38**, 883–891 (2020).
29. Wang, P., Xu, L., Gao, Y. & Han, R. BEON: A Functional Fluorescence Reporter for Quantification and Enrichment of Adenine Base-Editing Activity. Molecular therapy: the journal of the American Society of Gene Therapy **28**, 1696–1705 (2020).
30. Thuronyi, B.W. et al. Continuous evolution of base editors with expanded target compatibility and improved activity. Nature biotechnology **37**, 1070–1079 (2019).
31. Nioi, P. et al. Variant ASGR1 Associated with a Reduced Risk of Coronary Artery Disease. N Engl J Med **374**, 2131–2141 (2016).
32. Dalsgaard, T. et al. Improved Lentiviral Gene Delivery to Mouse Liver by Hydrodynamic Vector Injection through Tail Vein. Mol Ther Nucleic Acids **12**, 672–683 (2018).
33. Miao, C.H. et al. Inclusion of the hepatic locus control region, an intron, and untranslated region increases and stabilizes hepatic factor IX gene expression in vivo but not in vitro. Mol Ther **1**, 522–532 (2000).
34. Aronson, S.J. et al. Liver-directed gene therapy results in long-term correction of progressive familial intrahepatic cholestasis type 3 in mice. J Hepatol **71**, 153–162 (2019).
35. Shen, C.C. et al. Synthetic switch to minimize CRISPR off-target effects by self-restricting Cas9 transcription and translation. Nucleic Acids Res **47**, e13 (2019).
36. Bae, S., Park, J. & Kim, J.S. Cas-OFFinder: a fast and versatile algorithm that searches for potential off-target sites of Cas9 RNA-guided endonucleases. Bioinformatics **30**, 1473–1475 (2014).
37. Landrum, M.J. et al. ClinVar: public archive of interpretations of clinically relevant variants. Nucleic Acids Res **44**, D862-868 (2016).
38. Doman, J.L., Raguram, A., Newby, G.A. & Liu, D.R. Evaluation and minimization of Cas9-independent off-target DNA editing by cytosine base editors. Nat Biotechnol **38**, 620–628 (2020).
39. Antoniou, P., Miccio, A. & Brusson, M. Base and Prime Editing Technologies for Blood Disorders. Front Genome Ed **3**, 618406 (2021).
40. Zuo, E. et al. Cytosine base editor generates substantial off-target single-nucleotide variants in mouse embryos. Science **364**, 289–292 (2019).

41. Jang, H.K. et al. High-purity production and precise editing of DNA base editing ribonucleoproteins. Sci Adv **7** (2021).
42. Lyu, P. et al. Adenine Base Editor Ribonucleoproteins Delivered by Lentivirus-Like Particles Show High On-Target Base Editing and Undetectable RNA Off-Target Activities. CRISPR J **4**, 69–81 (2021).
43. Rees, H.A. et al. Improving the DNA specificity and applicability of base editing through protein engineering and protein delivery. Nat Commun **8**, 15790 (2017).
44. Jiang, T. et al. Chemical modifications of adenine base editor mRNA and guide RNA expand its application scope. Nat Commun **11**, 1979 (2020).
45. Qiu, M. et al. Lipid nanoparticle-mediated codelivery of Cas9 mRNA and single-guide RNA achieves liver-specific in vivo genome editing of Angptl3. Proc Natl Acad Sci U S A **118** (2021).
46. Stadelmann, C. et al. mRNA-mediated delivery of gene editing tools to human primary muscle stem cells. Mol Ther Nucleic Acids **28**, 47–57 (2022).
47. McGrath, E. et al. Targeting specificity of APOBEC-based cytosine base editor in human iPSCs determined by whole genome sequencing. Nat Commun **10**, 5353 (2019).
48. Berrios, K.N. et al. Controllable genome editing with split-engineered base editors. Nat Chem Biol **17**, 1262–1270 (2021).
49. Long, J. et al. A split cytosine deaminase architecture enables robust inducible base editing. FASEB J **35**, e22045 (2021).
50. Wang, X. & Musunuru, K. Angiopoietin-Like 3: From Discovery to Therapeutic Gene Editing. JACC Basic Transl Sci **4**, 755–762 (2019).
51. Stitziel, N.O. et al. ANGPTL3 Deficiency and Protection Against Coronary Artery Disease. J Am Coll Cardiol **69**, 2054–2063 (2017).
52. Fujimoto, K., Koishi, R., Shimizugawa, T. & Ando, Y. Angptl3-null mice show low plasma lipid concentrations by enhanced lipoprotein lipase activity. Exp Anim **55**, 27–34 (2006).
53. Chadwick, A.C., Evitt, N.H., Lv, W. & Musunuru, K. Reduced Blood Lipid Levels With In Vivo CRISPR-Cas9 Base Editing of ANGPTL3. Circulation **137**, 975–977 (2018).
54. El Refaey, M. et al. In Vivo Genome Editing Restores Dystrophin Expression and Cardiac Function in Dystrophic Mice. Circulation research **121**, 923–929 (2017).
55. Grose, W.E. et al. Homologous recombination mediates functional recovery of dysferlin deficiency following AAV5 gene transfer. PLoS One **7**, e39233 (2012).

Figures

Figure 1

Design and *in vitro* validation of self-inactivating ABE (siABE). (A) Predicted TadA8eW (8eW) domain structure. The C90 site was colored green. (B) Comparison of the editing efficiency of 8eW with or without the C90R mutation or C90-gRNA (C90-gR) at *Apoc3* in N2a cells. *ns*, not significant; one-way ANOVA with Turkey's multiple comparisons test. (C) Quantification of the siABE/C90-gR-induced editing at the C90 of 8eW. ****p<0.0001; two-tailed unpaired *t* test. (D) Schematic of the split siABE design. ITR, inverted terminal repeat sequence of AAV2; C90R, C90R-inducing gRNA; mhCMV, minimal CMV with muscle and heart enhancer; nCas9-N, Cas9 nickase split N terminal (2-573); nCas9-C, Cas9 nickase split C terminal (574-end); IntN, Gp41-1 intein N-terminal fragment; IntC, Gp41-1 intein C-terminal fragment; t-gR, targeting gRNA; pA, polyA signal. (E) Fluorescence microscopy images of HEK293 cells transfected with the reporter alone or the reporter plus the conventional split ABE (ABE-N/C) or the split siABE (siABE-N/C). Scale bar: 100 μm. (F, G) Flow cytometry analysis of EGFP expression (F) and measurement of the *mdx*^{4cv} target site editing efficiency (G) in HEK293 cells transfected as described in (E). *ns*, not significant; one-way ANOVA with Turkey's multiple comparisons test. (H) Time-course C90R editing efficiency with siABE-N/C. ****p<0.0001; one-way ANOVA with Turkey's multiple comparisons test. (I) *Apoc3* editing efficiency with ABE-N/C or siABE-N/C. *ns*, not significant; one-way ANOVA with Turkey's multiple comparisons test.

Figure 2

Design and *in vitro* validation of self-inactivating CBE (siCBE). (A) Schematic of the split siCBE design. Anc, AncBE4max; nCas9-N, Cas9 nickase split N terminal (2-713); nCas9-C, Cas9 nickase split C terminal (714-end); 2Ugi, 2 copies of uracil glycosylase inhibitor; si-gR, self-inactivating gRNA. (B) Quantification of the siCBE/Q125-gRNA-induced editing at the Q125 of AncBE4. ****p<0.0001; two-tailed unpaired *t* test. (C) Representative Western blot of AncBE4 expression in HEK293 cell lysates transfected with CBE-N/C or siCBE-N/C using the anti-Cas9 antibody. FL, the full-length AncBE4; N, the N-terminal fragment of AncBE4. (D) Densitometry quantification of relative full-length AncBE4 protein expression at different time points. *p<0.05, **p<0.01, ***p<0.001; two-tailed unpaired *t* test. (E) Time-course Q125X editing efficiency with siCBE-N/C. ****p<0.0001; one-way ANOVA with Turkey's multiple comparisons test. (F) Comparison of the editing efficiency of CBE-N/C and siCBE-N/C at the HEK4 site. ****p<0.0001, *ns*, not significant; one-way ANOVA with Turkey's multiple comparisons test.

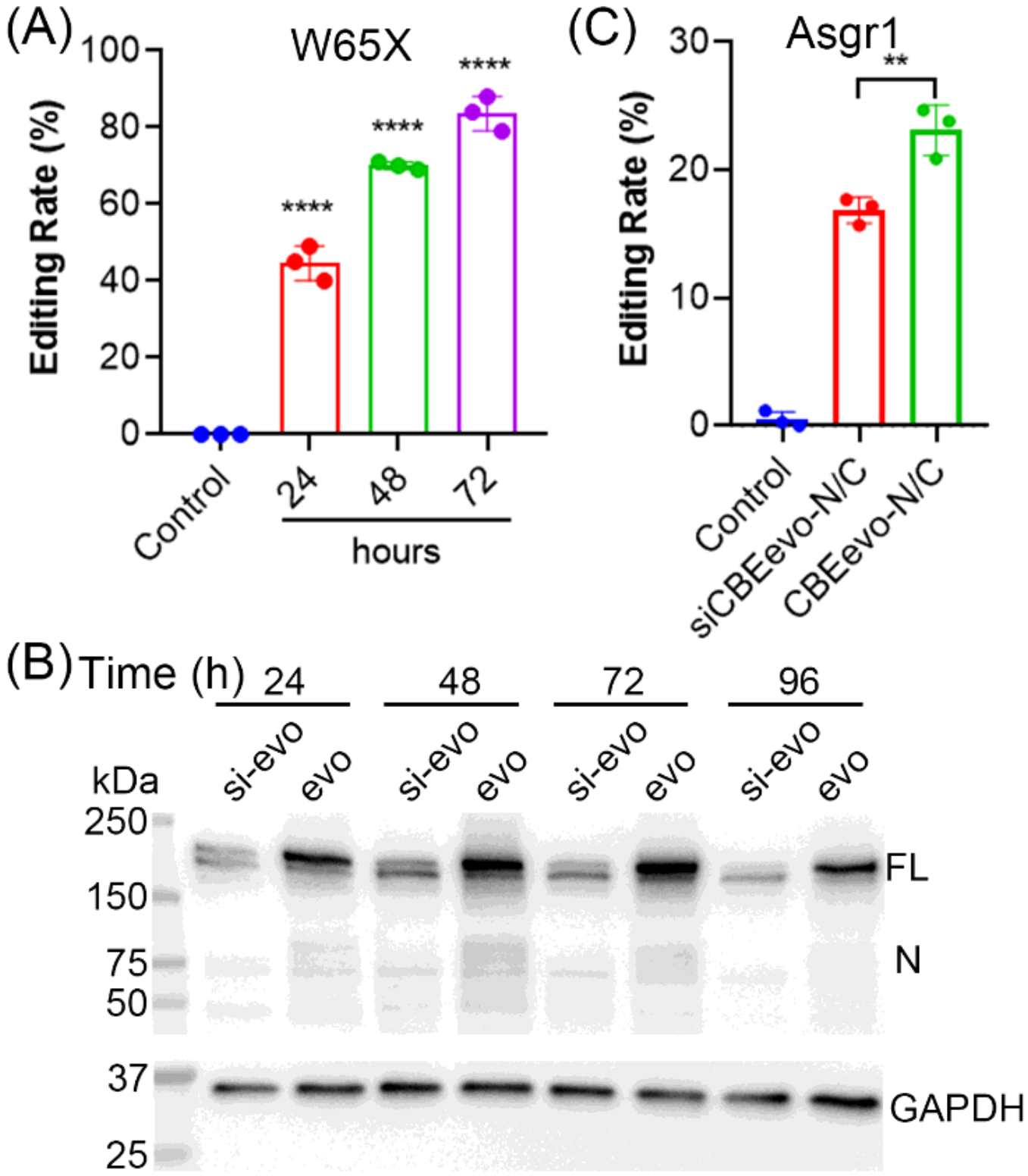

Figure 3

***In vitro* validation of self-inactivating CBE-evoFERNY (siCBEevo).** (A) Time-course editing efficiency of W65 codon on CBE-evoFERNY induced by siCBEevo-N/C in N2a cells. ****p<0.0001; one-way ANOVA with Turkey's multiple comparisons test. (B) Representative Western blot of CBE-evoFERNY expression in HEK293 cell lysates transfected with CBEevo-N/C or siCBEevo-N/C using the anti-Cas9 antibody. FL, the full-length CBE-evoFERNY; N, the N-terminal fragment of CBE-evoFERNY. (C) Comparison of the editing

efficiency of CBEevo-N/C (evo) and siCBEevo-N/C (si-evo) at mouse *Asgr1* locus. **p<0.01; one-way ANOVA with Turkey's multiple comparisons test.

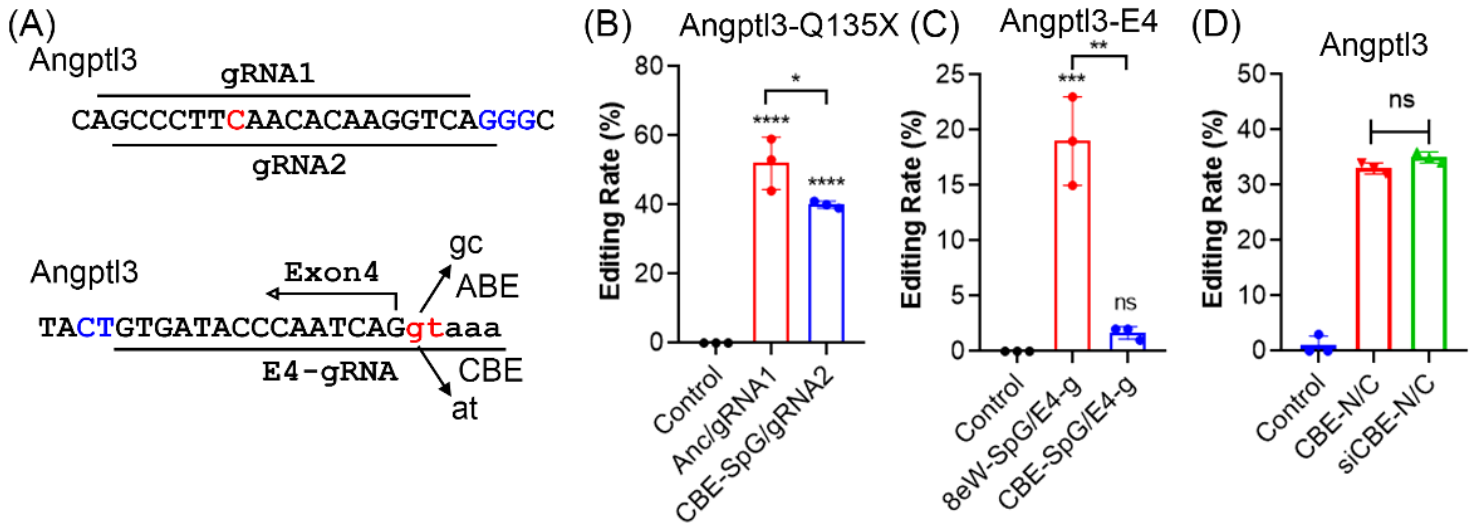

Figure 4

Generation of LoF mutations in mouse *Angptl3*. (A) Schematic of *Angptl3* gRNA designs. The targeted adenine or cytosine are colored in red and the PAM sequences are colored in blue. (B) Installation of Q135X mutation in mouse *Angptl3* induced by two overlapping gRNAs (gRNA1 and gRNA2) with different PAM-targeting CBEs (Anc or CBE-SpG). *p <0.05, ****p<0.0001; one-way ANOVA with Turkey's multiple comparisons test. (C) Measurement of base editing efficiency induced by *Angptl3*-E4-gRNA when combined with either ABE (8eW-SpG) or CBE (CBE-SpG). **p<0.01, ***p<0.001; one-way ANOVA with Turkey's multiple comparisons test. (D) Comparison of the editing efficiency of CBE-N/C and siCBE-N/C with *Angptl3*-gRNA1 to install Q135X mutation in mouse *Angplt3* in N2a cells. *ns*, not significant; one-way ANOVA with Turkey's multiple comparisons test.

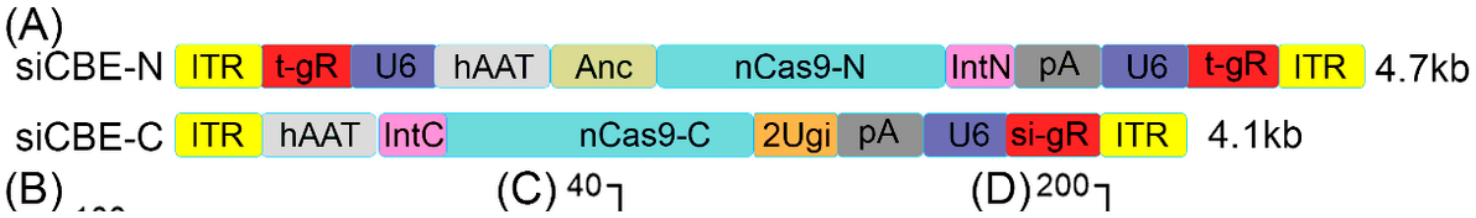

Figure 5

***In vivo* performance of AAV9-siCBE/Angptl3.** (A) Schematic of AAV9-siCBE/Angptl3 design. hAAT, human alpha-1-antitrypsin promoter. (B-D) Measurements of the serum levels of ANGPTL3 protein (B), TG (C) and TC (D) in mice at 1, 4 and 8 weeks after AAV9-si CBE/Angptl3 treatment. The control (Ctrl) mice received no treatments. *ns*, not significant; **p* <0.05, ***p*<0.01, ****p*<0.001 and *****p*<0.0001; one-way ANOVA with Turkey's multiple comparisons test. (E, F) Editing efficiency of *Angptl3* in the liver tissues of the mice treated with or without AAV9-siCBE/Angptl3, measured at the transcript (E) and genomic DNA (F) levels. ***p*<0.01, *****p*<0.0001; one-way ANOVA with Turkey's multiple comparisons test. (G) Western blot analysis of liver tissues collected from AAV9-siCBE/Angptl3 treated and control mice using anti-Cas9 antibodies. FL, full-length AncBE4; N, N-terminal fragment of AncBE4; G, Gapdh; Pos, positive control of HEK293 cell lysate transfected with siCBE-N/C plasmids.

Figure 6

Analysis of siCBE off-target activity. (A) Analysis of on-target and off-target DNA editing activities of CBE-N/C and siCBE-N/C with a pre-validated HEK4-gRNA in HEK293 cells. One-way ANOVA with Turkey's multiple comparisons test. (B, C) Analysis of on-target and off-target editing activities for Angptl3-gRNA1 (B) and self-targeting Q125-gRNA (C) in N2a cells. ND, not detectable. One-way ANOVA with Turkey's multiple comparisons test. (D, E) Analysis of on-target and off-target editing activities in mouse livers for Angptl3-gRNA1 (D) and self-targeting Q125-gRNA (E) following systemic delivery of AAV9-siCBE/Angptl3. One-way ANOVA with Turkey's multiple comparisons test.

Supplementary Files

This is a list of supplementary files associated with this preprint. Click to download.

- Plasmidsandprimersusedinthepaper.xlsx
- SupplementaryFigures.docx
- nrreportingsummary2022.pdf